Separation Science and Technology
Publication details, including instructions for authors and subscription information:
http://www.informaworld.com/smpp/title~content=t713708471

CO_2 Absorption Rate and Solubility in Monoethanolamine/Piperazine/Water

Hongyi Dang[a]; Gary T. Rochelle[a]
[a] Department of Chemical Engineering, The University of Texas at Austin, Austin, Texas, USA

Online publication date: 20 February 2003

To cite this Article Dang, Hongyi and Rochelle, Gary T.(2003) 'CO_2 Absorption Rate and Solubility in Monoethanolamine/Piperazine/Water', Separation Science and Technology, 38: 2, 337 — 357
To link to this Article: DOI: 10.1081/SS-120016678
URL: http://dx.doi.org/10.1081/SS-120016678

MARCEL DEKKER, INC. • 270 MADISON AVENUE • NEW YORK, NY 10016

SEPARATION SCIENCE AND TECHNOLOGY
Vol. 38, No. 2, pp. 337–357, 2003

CO_2 Absorption Rate and Solubility in Monoethanolamine/Piperazine/Water

Hongyi Dang and Gary T. Rochelle*

The University of Texas at Austin, Department of Chemical Engineering, Austin, Texas, USA

ABSTRACT

The solubility and absorption rate of carbon dioxide into monoethanolamine/piperazine/water were measured in a wetted wall column at 40–60°C. The total amine concentration was varied from 1.0 M to 5.0 M, with monoethanolamine blends containing 0 to 1.2 M piperazine. CO_2 solubility and solution speciation were simulated by nine equilibrium reactions. Two of the equilibrium constants were adjusted to match literature data. The rate of absorption was predicted by the theory of diffusion with fast chemical reaction. Piperazine at 24 mol% of the total amine decreases CO_2 equilibrium pressure by 50% and enhances the CO_2 absorption rate by 50% to 100%. The CO_2 enhancement factor decreases by a factor of 0.6 to 2 as loading decreases from 0 to 0.5 mol CO_2/mole amine.

*Correspondence: Gary T. Rochelle, The University of Texas at Austin, Department of Chemical Engineering, Austin, TX 78712, USA; Fax: 512-475-7824; E-mail: Rochelle@che.utexas.edu.

DOI: 10.1081/SS-120016678 0149-6395 (Print); 1520-5754 (Online)

MARCEL DEKKER, INC. • 270 MADISON AVENUE • NEW YORK, NY 10016

Key Words: Monoethanolamine; Piperazine; Carbon Dioxide; Absorption.

INTRODUCTION

Aqueous monoethanolamine (MEA) is widely used for removing carbon dioxide (CO_2) from natural gas streams and refinery process streams. It is also used to remove CO_2 from combustion gases and may receive wide application for abatement of greenhouse gases. MEA is a relatively strong base with a fast reaction rate, yielding a low CO_2 concentration. A number of investigators have studied the solubility[1–4] and reaction kinetics[5–9] of CO_2 in aqueous MEA.

Even though MEA reacts relatively fast with CO_2, the rate of absorption is still controlled by reaction kinetics. Typical absorber tray efficiency is less than 20%. Piperazine (PZ) was studied as a promoter for methyldiethanolamine (MDEA) by Xu et al.[10–12] and Kaganoi.[13] Bishnoi[14] determined that the rate constant of PZ with CO_2 is one order of magnitude higher than that of MEA with CO_2. Therefore, a blend of MEA/PZ should absorb CO_2 faster than MEA alone.

The objective of this work is to quantify the effectiveness of PZ as a rate promoter in aqueous MEA. The solubility and absorption rate of CO_2 in MEA/PZ/H_2O have been measured in loaded and lean solutions with a wetted wall column. The results are compared with the predictions of a simple vapor–liquid equilibrium model and a simple rate model.

EXPERIMENTAL APPARATUS AND METHODS

The wetted wall column (Fig. 1) was constructed from a stainless steel tube with a well-defined surface area (38.52 cm^2) and a characteristic liquid film mass transfer coefficient similar to that of a packed tower. The stainless steel tube was 9.1 cm long and had an outside diameter of 1.26 cm. Liquid overflowed from the inside and formed a liquid film over the outer surface of the stainless steel tube. Gas entered the wetted wall column from the bottom and countercurrently contacted the liquid film. Figure 2 shows the overall flow diagram of the apparatus used in this study to obtain solubility and absorption rate data. The apparatus was originally built by Mshewa[15] and modifications were made by Pacheco et al.[16,17] More details are given by Dang.[18]

Flow from two gas cylinders was regulated by Brooks model 5850E mass flow controllers. The gas was presaturated at the same temperature as

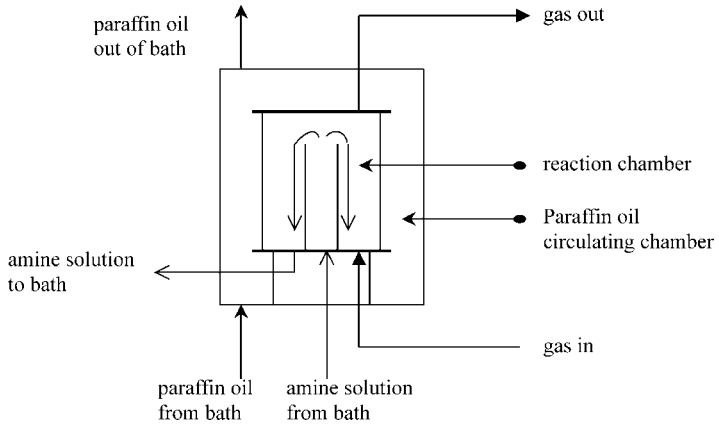

Figure 1. Detailed column diagram.

the wetted wall column. The total pressure used in this work was around 4 to 5 atm. To minimize gas film resistance, the gas flow rate was approximately 5 to 6 SLPM.

The gas was sent from the column through a needle valve where the pressure was reduced to atmospheric. From the downstream side of the needle valve, the gas was sent to a condenser that consisted of an Erlenmeyer flask submerged in ice water. The gas was then passed on to a series of Horiba PIR

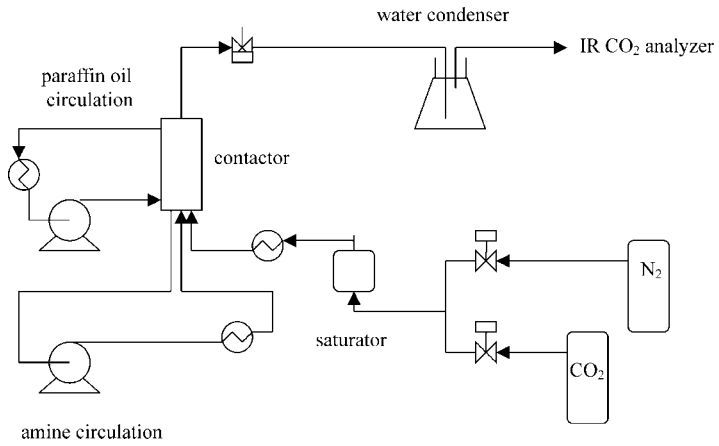

Figure 2. Overall experimental flowsheet.

2000 carbon dioxide analyzers where the outlet carbon dioxide concentration was measured by infrared spectroscopy. Two analyzers were used, each having a different concentration range (0–25% and 0–0.25%, volume basis).

The amine solution was kept in a reservoir and passed through a coil submerged in an oil bath to heat it to the reactor temperature. Anhydrous piperazine (99.9%) from Aldrich Chemical and MEA from a commercial supplier were mixed with deionized water to make up the amine solution. The flow of amine solution was provided by a Cole-Parmer micropump and was measured by a liquid rotameter. The liquid flow rate was 3 cm^3/s. A reservoir with a 400 cm^3 holdup was used for the amine solution. The paraffin oil in the bath was also circulated to the wetted wall column, keeping the entire apparatus at a uniform temperature. The inlet and outlet temperatures of the amine solution were measured (typically with a difference of 1°C to 2°C) and the temperature in the column was approximated by the average of the inlet and outlet temperatures.

Absorption or desorption of CO_2 was determined from the gas phase material balance using the measured inlet and outlet gas concentrations. Periodically, liquid samples were withdrawn from a sample port close to the reactor outlet and analyzed for total carbon dioxide by acidic evolution into a CO_2 analyzer.[13,15–17,19] Amine solution was also added or withdrawn periodically from the sample port to keep the liquid level constant in the wetted wall column.

PHYSICAL PARAMETERS

Table 1 gives the methods for calculating the physical parameters. The Henry's constant was calculated as a function of amine concentration, but not of CO_2 loading. A more rigorous model of absorption rate should also include a dependence on loading. The expressions for k_1^0 and k_g were developed by previous investigators with CO_2 desorption from water and SO_2 absorption respectively.

DATA ANALYSIS AND EXPERIMENTAL RESULTS

In this work, at any given loading for a particular amine solution, both absorption and desorption rates were measured by variation of CO_2 partial pressure around the equilibrium partial pressure. When the flux is equal to zero, the partial pressure of CO_2 will be the equilibrium partial pressure of CO_2 at that loading. This point can be found by bracketing the absorption and

Table 1. Methods for calculation of physical parameters.

Property	Formula	Comment
ρ (g/mL)	$\rho = (X_{Am}M_{AM} + X_{H2O}M_{H2O} + X_{CO2}M_{CO2})/V$	Includes correction in V for solution nonideality[23]
μ (uPa-S)	$\mu/\mu_{H2O} = \exp\{[(a\Omega + b)T + (c\Omega + d)][\alpha(e\Omega + f\,T + g) + 1]\Omega T^2)\}$	[23]
H [atm/(mol-L)]	$H_{CO2,MEA} = R*\exp[-2625/T + 12.2]$ $R = \exp[(A/T + B)X_1 + hI]$	hI term was neglected in this work[24]
D (m^2/s)	N_2O analogy	Stokes–Einstein relation was used for D_{N2O}, amine[25]
k_l^0 (cm/s)	$k_l^0 = QL(1 - \Theta)/a$	[26]
k_g (mol/(Pa·cm^2/s)	$Sh = 1.075(Re{\cdot}Sc{\cdot}d/h)^{0.85}$	[14]

desorption rates. Figure 3 gives an example of 5.0 M MEA with 0.299 mol CO_2/mol MEA. While inferring the equilibrium partial pressure, only measurements close to equilibrium were considered.

By applying the same method to every loading, we determined CO_2 equilibrium partial pressure at a number of solution compositions (Table 2).

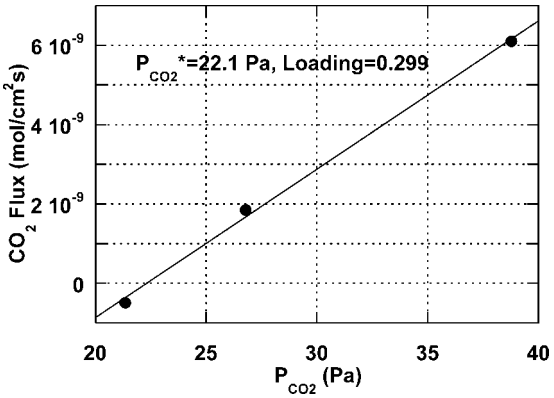

Figure 3. Extraction of CO_2 solubility in 5.0 M MEA at 40°C, P^*_{CO2} = 22.1 Pa, 0.299 mol CO_2/mol amine.

Table 2. Measured and predicted enhancement factors for CO_2 absorption in MEA/PZ/H_2O.

	Amine (M)			P^*_{CO2} (Pa)										
T (°C)	MEA	PZ	Ldg	exp	model	$k'_G \cdot 10^{10a}$	k_1^0 (cm/s)	E_{exp} [a]	E_{pred}	E_1	E_{inst}	k_G/k_g	$\frac{P_i - P^*}{P}$	Removal (%)
60	0.4	0.6	0.057	18.2	1.5	4.70	0.016	174	136	137	21900	0.68	0.29[b]	42.4
			0.14	115	13	2.88	0.016	107	117	120	5090	0.54	0.26[b]	39
	2.5	0	0.091	27.6	4.6	3.18	0.015	120	98.4	98.7	38000	0.56	0.39	38.7
			0.33	254	300	1.54	0.015	58.5	72	73	4020	0.31	0.62	25
			0.614	7730	49000	0.54	0.015	20.4	16	28	38	0.19	0.25[b]	5.9[b]
	1.9	0.6	0.01	0.2	0.02	7.19	0.015	272	181	182	275000	0.73	0.27[b]	52.2
			0.21	102	56.4	3.14	0.014	127	144	145	12900	0.56	0.43	53.9
			0.44	2420	1500	1.46	0.013	64	74	87	480	0.39	0.31	31.1
	5.0	0	0.27	224	116	2.42	0.012	104	124	125	7310	0.48	0.42	32.5
			0.52	9550	20000	0.44	0.011	20.6	33	55	84	0.14	0.55	8.4[b]
	3.8	1.2	0.41	518	1003	2.96	0.011	140	172	183	2570	0.54	0.36	34.4
40	5.0	0	0.30	22.1	29	2.00	0.0085	92	101	101	76800	0.43	0.51	32.1
			0.47	768	852	0.42	0.0078	20.8	32	36	280	0.14	0.78	11.5[b]
	3.8	1.2	0.43	90.5	118	2.04	0.0073	109	122	123	16600	0.44	0.35	24.3

Ldg: loading (mol CO_2/mol amine); k'_g [mol/(cm^{2}s*Pa)]: normalized flux = flux/($P_{CO2,i} - P_{CO2}$*); k_1^0 : liquid phase mass transfer coefficient; E_{exp}: measured enhancement factor; E_{pred}: predicted enhancement factor; E_1: predicted pseudo first-order enhancement factor; E_{inst}: instantaneous enhancement factor; exp: measured value; model: predicted value.

[a] Values are calculated by using measured CO_2 equilibrium partial pressure, P^*_{CO2}.

[b] These parameter values are indicative of potential uncertainty in k'_G.

In the mass transfer process between the gas phase and the liquid phase, which is enhanced by chemical reactions, the total resistance to mass transfer was modeled as the sum of gas film ($1/k_g$) and liquid film resistance ($1/k'_G$) :

$$\frac{1}{k_g} + \frac{1}{k'_G} = \frac{1}{K_G} \tag{1}$$

The total gas phase mass transfer coefficient, K_G, was calculated by the following expression.

$$K_G = \frac{\text{Flux}}{P_{CO_2} - P^*_{CO_2}} \tag{2}$$

where, P_{CO2} is the operational partial pressure of CO_2 in the wetted wall column, which was calculated by the log mean average:

$$P_{CO_2} = \frac{P_{CO_2,in} - P_{CO_2,out}}{\text{Ln}\left(P_{CO_2,in}/P_{CO_2,out}\right)} \tag{3}$$

The liquid phase mass transfer coefficient with chemical reactions, k'_G, was calculated by

$$k'_G = \frac{\text{Flux}}{(P_{CO_2,i} - P^*_{CO_2})} \tag{4}$$

where, P^*_{CO2} is equilibrium partial pressure of CO_2, which is measured by bracketing both absorption and desorption data near equilibrium. The partial pressure of CO_2 at the gas liquid interface, $P_{CO2,i}$, is calculated by

$$P_{CO_2,i} = P_{CO_2} - \frac{\text{Flux}}{k_g} \tag{5}$$

k_g is calculated by the equation given in Table 1.[14] k'_G can also be expressed as:

$$\frac{1}{k'_G} = \frac{H}{k^0_1 E} \tag{6}$$

where, E is the enhancement factor, which is defined as the ratio of flux with chemical reactions to that without chemical reactions.

In Table 2, six points have been identified that may have greater uncertainty. The uncertainty in the calculated value of E or k'_G is indicated by low values of the fraction removal of CO_2, $(P_{CO2,in} - P_{CO2,out})/P_{CO2,in}$, and the approach to equilibrium, $(P_i - P^*)/P$. Low removal of the CO_2 ($<20\%$) causes great uncertainty because the flux is determined as the difference

between inlet and outlet concentrations. A small approach to equilibrium (<0.3) at the interface causes great uncertainty in the estimate of the driving force and includes the effect of a high gas film resistance. Estimates of P^*_{CO2} are especially important with a small approach to equilibrium.

At each loading in a given amine concentration, the CO_2 partial pressure was varied to obtain a series of rate data. CO_2 flux is plotted versus liquid driving force ($P_{CO2,i} - P^*_{CO2}$) to obtain a straight line. k'_G can be obtained from the slope of this straight line. Then E is calculated from Eq. 6. The measured rate data are summarized in Table 2. The detailed data and error analysis are given in Dang et al.[18]

SOLUBILITY AND SPECIATION MODEL

In the VLE model, one phase equilibrium and 5 chemical equilibria in the liquid phase were considered for CO_2/MEA/H_2O.

$$CO_2(aq) \overset{H_{CO_2}}{\leftrightarrow} CO_2(g) \tag{7}$$

$$2H_2O \overset{K_{H_2O}}{\leftrightarrow} H_3O^+ + OH^- \tag{8}$$

$$2H_2O + CO_2 \overset{K_{a,CO_2}}{\leftrightarrow} H_3O^+ + HCO_3^- \tag{9}$$

$$H_2O + HCO_3^- \overset{K_{a,HCO_3^-}}{\leftrightarrow} H_3O^+ + CO_3^{2-} \tag{10}$$

$$H_2O + MEAH^+ \overset{K_{a,MEA}}{\leftrightarrow} H_3O^+ + MEA \tag{11}$$

$$H_2O + MEA + CO_2 \overset{K_{a,MEACOO^-}}{\leftrightarrow} H_3O^+ + MEACOO^- \tag{12}$$

There are three material balance equations for CO_2, MEA, and the whole solution respectively,

$$X_{CO_{2,T}} = X_{CO_2} + X_{HCO_3^-} + X_{CO_3^{2-}} + X_{MEACOO^-} \tag{13}$$

$$X_{MEA,T} = X_{MEA} + X_{MEAH^+} + X_{MEACOO^-} \tag{14}$$

$$\sum X_i = 1 \tag{15}$$

Because the solution is neutral, there exists a charge balance:

$$0 = 2X_{CO_3^{2-}} + X_{HCO_3^-} + X_{OH^-} + X_{MEACOO^-} - X_{H_3O^+} - X_{MEAH^+} \tag{16}$$

Table 3. Comparison of literature values to model parameters fitted to data from Jou.[1]

	K_a (fitted)	K_a [27]	K^-_{MEACOO} (fitted)	K^-_{MEACOO} [27]
5.0 M MEA, 60°C	$9.18E-12$	$1.45E-11$	$5.84E-6$	$2.87E-5$
5.0 M MEA, 40°C	$1.26E-12$	$3.51E-12$	$5.03E-6$	$5.51E-5$

Assuming that the Henry's law constant and the equilibrium constants of the chemical reactions are available, the equilibrium partial pressure of CO_2 in the gas phase and the mole fractions of each species in the liquid phase can be calculated. However, the literature values for the reaction equilibrium constants are for infinite dilution in water. In this work, the amine solution is concentrated and the strong ionic effects will change the system behavior. This work uses the literature values of the water dissociation constant, CO_2 dissociation constant, and HCO_3^- dissociation constant from Maurer[20] and Edwards et al.[21] respectively, and it adjusts the pK_a value of MEA [reaction (15)] and the carbamate stability constant of MEA [reaction (16)], to account for the all of the nonideality of the system.

The solubility data of CO_2 in 5 M MEA at 60°C and 40°C of Jou et al.[1] were used to determine the two model parameters of the VLE model at 60°C and 40°C, respectively. The parameters are listed in Table 3 and the literature values for the other equilibrium constants are listed in Table 4. Because these equilibrium constants were defined in terms of mole fraction and activity coefficients, they are dimensionless. Figure 4 shows the result of the parameter fitting with the measured solubility data.

By introducing the following three chemical reactions, the VLE model was expanded to CO_2/MEA/PZ with the equilibrium constants from Bishnoi

Table 4. Temperature dependence of the equilibrium constants.

$\mathrm{Ln\,K} = C_1 + C_2/\mathrm{T(K)} + C_3 \mathrm{Ln\,T(K)}$

Reaction	C_1	C_2	C_3	Source
K_{H2O}	132.899	−13445.9	−22.4773	Maurer[20]
$K_{a,CO2}$	231.465	−12092.1	−36.7816	Edwards et al.[21]
$K^-_{a,HCO3}$	216.049	−12431.7	−35.4819	Edwards et al.[21]
$K_{a,PZ}$	−11.91	−4350.6	0	Bishnoi et al.[22]
K^-_{PZCOO}	−29.308	5614.64	0	Bishnoi et al.[22]
$K_{PZ(COO-)2}$	−30.777	5614.64	0	Bishnoi et al.[22]

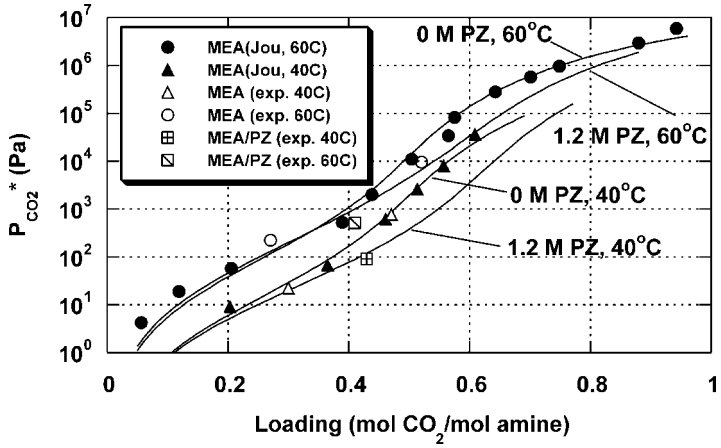

Figure 4. CO_2 solubility in 5 M amine (MEA + PZ) at 60°C and 40°C, predicted by parameters in Table 3, data from Jou.[1]

et al.[22] listed in Table 4.

$$H_2O + PZH^+ \overset{K_{a,PZ}}{\longleftrightarrow} H_3O^+ + PZ \tag{17}$$

$$H_2O + PZ + CO_2 \overset{K_{PZCOO^-}}{\longleftrightarrow} H_3O^+ + PZCOO^- \tag{18}$$

$$H_2O + PZCOO^- + CO_2 \overset{K_{PZ(COO^-)_2}}{\longleftrightarrow} H_3O^+ + {}^- OCPZCOO^- \tag{19}$$

The predicted speciation of CO_2 in 1.9 M MEA/0.6 M PZ at 60°C, and in 3.8 M MEA/1.2 M PZ by this model is shown in Figs. 5 and 6.

Figure 7 compares values of the equilibrium CO_2 partial pressure normalized by the value predicted by the model for 5 M MEA without piperazine. At 40°C and 60°C, the model prediction for 5 M MEA and the data by Jou and Mather[1] match each other reasonably well at moderate loading, but differ as much as a factor of three at very low and very high loading. Our two experimental points for 5 M MEA at 40°C match the model well, but our two experimental points at 60°C differ from the model by a factor of two.

In Fig. 7, both calculated curves and our measured data indicate that the addition of PZ to MEA can decrease the CO_2 equilibrium partial pressure by a factor of 2–5 at medium and high loading, but has no significant effect at low loading.

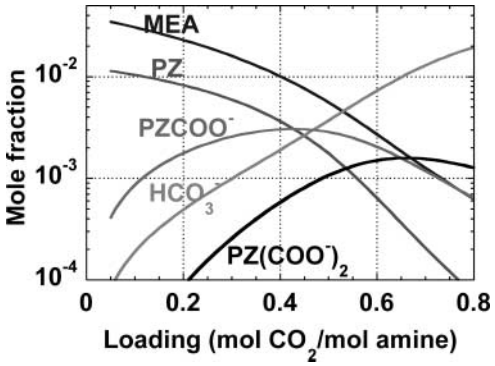

Figure 5. Predicted speciation of CO_2 in 1.9 M MEA/0.6 M PZ at 60°C.

RATE MODEL

This work uses a simple rate model to predict the enhancement factor, *E*, for CO_2 absorption in MEA/PZ/H_2O. The model includes two contributions: pseudo first-order enhancement and instantaneous enhancement.

Pseudo First-Order Enhancement Factor

In the CO_2/MEA/PZ/H_2O system, three finite-rate, reversible reactions, 12, 18, and 19, are important. If the MEA, PZ, and $PZCOO^-$ concentration

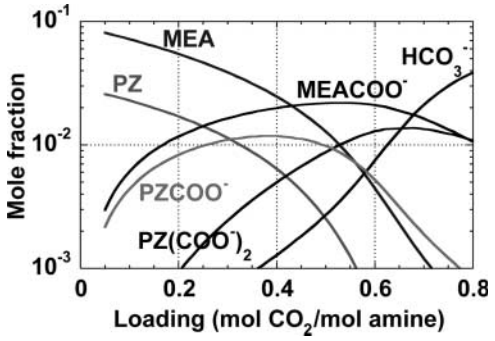

Figure 6. Predicted speciation of CO_2 in 3.8 M MEA/1.2 M PZ at 40°C.

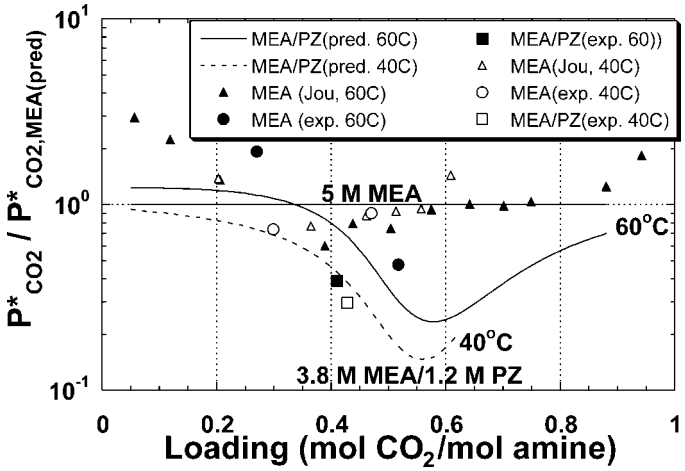

Figure 7. Comparison of predicted CO_2 solubility, literature data, and experimental data in 5.0 M MEA blends with 0 or 1.2 M PZ at 60°C and 40°C. $P^*_{CO2,\,MEA(pred)}$ is calculated using the constants from Table 3.

gradients in the liquid film are neglected and represented by their bulk values respectively, the analytical expression for the pseudo first-order enhancement factor, E_1, with fast reaction rates is given by:

$$E_1 = \frac{\sqrt{(k_{MEA}[MEA] + k_{PZ}[PZ] + k_{PZCOO^-}[PZCOO^-])D_{CO_2}}}{k_l^0} \tag{20}$$

With the assumption of pseudo first-order, [MEA], [PZ], and [$PZCOO^-$] are the concentrations of these species in the bulk solution. k_{MEA}, k_{PZ}, and k^-_{PZCOO} are the second order rate constants of MEA, PZ, and $PZCOO^-$ with CO_2, respectively. k_{MEA} and k_{PZ} were calculated by Eqs. 21[8] and 22.[14]

$$\log_{10}(0.001 * k_{MEA}(m^3/mole{\cdot}s)) = 10.99 - 2152/T(K) \tag{21}$$

$$k_{PZ}(m^3/mol{\cdot}s) = 0.001 * k_{25°C} \exp\left[\frac{-\Delta H_a}{R}\left(\frac{1}{T(K)} - \frac{1}{298}\right)\right] \tag{22}$$

where, $k_{25°C} = 5.37E_4\ m^3/kmol$, $\Delta H_a = 3.36E_4\ kJ/kmol$.

Because the K_a of $PZCOO^-$ is about four times greater than that of PZ,[14] k_{PZCOO^-} was assumed to be one fourth of k_{PZ}. In this work, the liquid film mass transfer coefficient, k_1^0, varies from $0.8E-4$ to $1.6E-4$ m/s.

Instantaneous Enhancement Factor

To account for the potentially limiting diffusion of reactants and products on the mass transfer process, the simple model includes an estimate of the instantaneous enhancement flux:

$$\text{flux}_{\text{phy}} = \frac{k_{1,CO2}}{H_{CO2}}(P_{CO2,1} - P^*_{CO2,b}) \tag{23a}$$

$$\text{flux}_{\text{inst}} = k_{1,\text{prod}}(\text{loading}_i - \text{loading}_b)C_{\text{amine}} \tag{23b}$$

The instantaneous enhancement factor is given by the ratio of Eqs. 23b and 23a with the substitution of the ratio of the square root of the diffusivities for the ratio of the liquid film mass transfer coefficients:

$$E_{\text{inst}} = C_{\text{amine}}\, H_{CO_2} \frac{\Delta(\text{loading})}{\Delta(P^*_{CO_2})} \sqrt{\frac{D_{CO_2}}{D_{\text{product}}}} \tag{23}$$

If the flux and ΔP^*_{CO2} across the interface are small, Eq. 23 reduces to:

$$E_{\text{inst}} = C_{\text{amine}}\, H_{CO_2} \frac{\partial(\text{loading})}{\partial(P^*_{CO_2})} \sqrt{\frac{D_{CO_2}}{D_{\text{product}}}} \tag{24}$$

The derivative of the equilibrium loading with equilibrium partial pressure was determined numerically from the results of the VLE model. This means that E_{inst} is a global instantaneous enhancement factor that assumes that the reactions of MEA, PZ, and $PZCOO^-$ with CO_2 are all instantaneous. The ratio of D_{CO2} to D_{product} was approximated by a value of 2.0.

Total Enhancement Factor

The simple model is completed by assuming a series resistance. This model will account for the effects of equilibrium and the instantaneous enhancement factor at high loading. If the reaction occurs near the interface, then reaction enhancement E_1 is in series with instantaneous enhancement E_{inst}.

$$\frac{1}{E} = \frac{1}{E_1} + \frac{1}{E_{\text{inst}}} \tag{25}$$

Equation 25 can also be derived by combining equations 26, 27, and 28 as

a simple series resistance in the driving force for CO_2:

$$\text{flux} = E_1([CO_2]_i - [CO_2]_i^*)k_1^0 \quad (26)$$

$$\text{flux} = E_{inst}([CO_2]_i^* - [CO_2]_b^*)k_1^0 \quad (27)$$

$$\text{flux} = E([CO_2]_i - [CO_2]_b^*)k_1^0 \quad (28)$$

RESULTS

Table 2 and Figs. 8 through 10 compare the measured and calculated CO_2 absorption rate. The predictions agree well with the measured data at medium loading in 1.0 M MEA/PZ blends and 2.5 M MEA/PZ, but overestimate the rate for 5.0 M MEA/PZ blends at both 40°C and 60°C.

Both the calculated and the measured data show that 0.6 M PZ in 1.0 M MEA increases the rate by a factor of 2 to 2.5 at 60°C. The addition of 0.6 M PZ to 2.5 M MEA and 1.2 M PZ to 3.8 M MEA increase the rate by a factor of 1.5 to 2 at 40°C and 60°C.

The relative effect of PZ ($E_{MEA/PZ}/E_{MEA}$) is practically independent of CO_2 loading, except at very high loading. This is because $PZCOO^-$ is also a reactive species with CO_2. Only at very high loading (0.8–0.9), are both PZ and $PZCOO^-$ depleted.

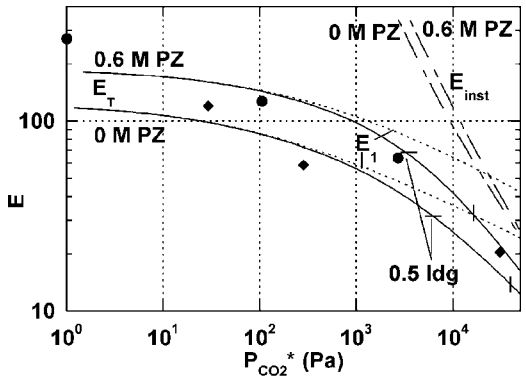

Figure 8. CO_2 absorption rate in 2.5 M amine with 0 or 0.6 M PZ at 60°C, curves predicted by the rate model with $D_{CO2} = 4.11E - 5\,cm^2/s$, $k_{MEA} = 3.37E4\,L/mol\text{-}s$, $k_{PZ} = 2.23E5\,L/mol\text{-}s$, $k_{PZCOO^-} = 5.58E4\,L/mol\text{-}s$, $k_1^o = 0.015\,cm/s$. The experimental data are circles for 0.6 M PZ and diamonds for 0 M PZ.

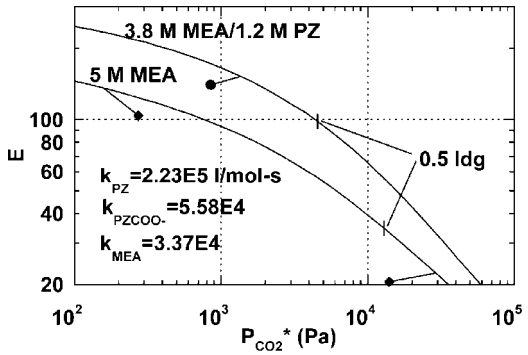

Figure 9. CO_2 absorption rate in 5.0 M amine with 0 or 1.2 M PZ at 60°C, curves predicted by the rate model with the listed constants, line segments connect values of equal loading.

In both MEA/PZ and MEA solvents, when the loading of lean solutions increases to 0.5 mol CO_2/mol amine, the enhancement factors decrease by a factors of 2 to 3. This is because of the consumption of the reactive species with loading.

The simple rate model (see Figs. 9 and 10) indicates that at higher temperature, both MEA and MEA/PZ have higher rates than at lower temperature. There is no significant difference in the relative effect of PZ ($E_{MEA/PZ}/E_{MEA}$) between 40°C and 60°C.

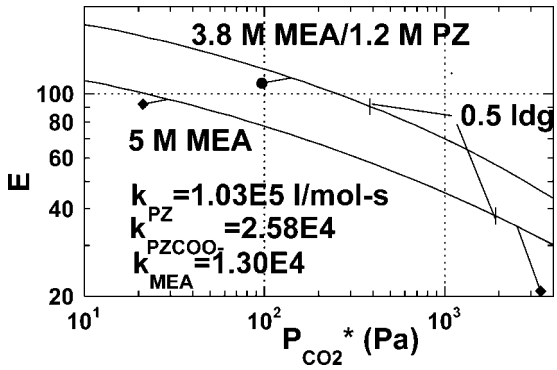

Figure 10. CO_2 absorption rate in 5.0 M amine with 0 or 1.2 M PZ at 40°C, curves predicted by the rate model with the listed constants, line segments connect values of equal loading.

Rate Contributions of Important Species

The speciation of the amine solution plays a very important role in the CO_2 absorption rate. The contributions of three important species in MEA/PZ blends (MEA, PZ, and $PZCOO^-$) to the total absorption rate are compared in Fig. 11. The rate fraction of each species is calculated as:

$$\text{rate fraction of species i} = k_i[i]/(k_{MEA}[MEA] + k_{PZ}[PZ] + k_{PZCOO^-}[PZCOO^-]) \quad (29)$$

where, k_i is the rate constant of species i (MEA, PZ, and $PZCOO^-$) with CO_2 as given by Eqs. 21 and 22. K_{PZCOO^-} is assumed to be 25% of k_{PZ}. $[i]$ is the concentration of each species calculated by the VLE model of this work.

Figure 11 shows the rate fractions of MEA, PZ, and $PZCOO^-$ in 3.8 M MEA/1.2 M PZ at 60°C. At loading less than 0.5, PZ contributes more than 50% of the total absorption rate. When the loading is higher than 0.65, $PZCOO^-$ contributes more than 50% of the total reaction rate. MEA contributes 20–30% of the rate throughout the range of loading.

The contribution of $PZCOO^-$ is only important at high loading because we have assumed that $k_{PZCOO^-} = 0.25\,k_{PZ}$. We saw little effect of k_{PZCOO^-} when it was reduced to 10% of k_{PZ}.[18] In modeling of data for MDEA/PZ, Bishnoi[19] used $k^-_{PZCOO} \approx k_{PZ}$. However, there was still a large uncertainty in the estimate of k^-_{PZCOO}.

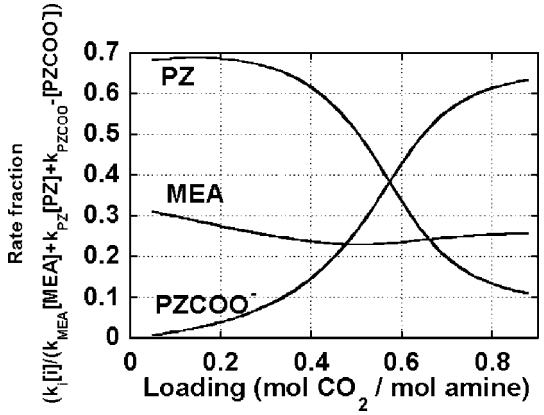

Figure 11. Contributions of reactive amine species to the CO_2 reaction rate in 3.8 M MEA/1.2 M PZ at 60°C.

Effect of Reactant and Product Diffusion

The pseudo first-order enhancement factor accounts for the effect of chemical reactions on the CO_2 absorption rate, but it does not account for reactant depletion or product accumulation at the gas–liquid interface. In Fig. 8, the two types of dashed lines show the significance of the pseudo first-order and instantaneous contributions to the enhancement factor. With loading less than 0.5 mol CO_2/mol amine, the pseudo first-order model represents the overall enhancement accurately. At higher loading, instantaneous enhancement becomes important and even dominant. The instantaneous enhancement factor in MEA and MEA/PZ is almost identical, therefore, the difference in kinetics accounts for the promotion of CO_2 absorption by PZ in MEA solution.

Amine Depletion at the Gas–Liquid Interface

In this study, the rate model combines as series resistances the estimated values of the pseudo first-order and instantaneous enhancement factor. The estimation of the instantaneous enhancement factor assumes that there is a low driving force and flux. The combination of the resistances assumes that there is no depletion of amine at the gas–liquid interface. Neither of these assumptions is good with the measurements at high loading, usually made with a large driving force and a large flux. Therefore, a more rigorous model would be more accurate in predicting the enhancement at high loading.

CONCLUSION

The absorption rate of CO_2 at 40°C and 60°C in aqueous MEA with 0.6 to 1.2 M PZ is 1.5–2.5 times greater than that in MEA alone.

In both MEA and MEA/PZ solvents, the CO_2 enhancement factor is 2 to 3 times smaller in rich solutions (0.5 mol CO_2/mol amine) than in lean solutions. Therefore, a larger fraction of the absorber packing height will be devoted to mass transfer under rich conditions. This effect results from the depletion of MEA and PZ at greater loading.

With less than 0.4 mol CO_2/mol amine, the PZ species contributes more than 60% of the total absorption rate. With loading more than 0.6 mol CO_2/mol amine, the species $PZCOO^-$ accounts for more than 40% of total absorption rate. For most of the cases studied in this work, MEA has a 20% to 30% contribution to the total absorption rate over the whole range of loading.

At 40°C and 60°C, and loading greater than 0.4 to 0.5 mol CO_2/mol amine, the equilibrium partial pressure of CO_2 in aqueous MEA with 0.6 to 1.2 M PZ is 2 to 5 times smaller than with MEA alone. At loading less than 0.2 to 0.3, there is no significant effect of PZ on the equilibrium partial pressure of CO_2.

The effects of PZ, CO_2 loading, and temperature are predicted well by the simple model combining estimated values of the pseudo first-order and instantaneous enhancement factors. This simple model predicts accurate values of the enhancement factors in 1.0 and 2.5 M amine, but overpredicts the enhancement in 5.0 M amine by 10 to 80%. A more rigorous simulation of reactant and product diffusion may be necessary at these conditions.

NOMENCLATURE

d	hydraulic diameter of the wetted wall column (m)
D	diffusion coefficient (m^2/s)
E	enhancement factor
h	height of the wetted wall column (m)
H	Henry's law constant (Pa^{-1})
I	ionic strength
k	rate constant (m^3/mol s)
k_g	gas film mass transfer coefficient [mol/(Pa·cm^2·s)]
k_G	mass transfer coefficient based on gas phase [mol/(Pa·cm^2·s)]
k_l^0	liquid film mass transfer coefficient (m/s)
K	Equilibrium constant
M	molecular weight
P_x	partial pressure of x (Pa)
Q_L	flow rate (m^3/s)
Re	Reynolds number
Sc	Schmidt number
Sh	Sherwood number
T	Temperature (K)
V	volume of solution (m^3)
X	mole fraction
α	CO_2 loading (mol CO_2/mol amine)
Θ	parameter to calculate mass transfer coefficient
μ	viscosity (Pa·s)
ρ	density (kg/m^3)
Ω	mass percent of amine

*Units are as above without specific definition.

ACKNOWLEDGMENTS

This work was supported by the Separations Research Program at the University of Texas and other industrial sponsors.

REFERENCES

1. Jou, F.-Y.; Mather, A.E.; Otto, F.D. The solubility of CO_2 in a 30 mass percent monoethanolamine solution. Can. J. Chem. Eng. **1995**, *73*, 140–147.
2. Lee, J.I.; Otto, F.D.; Mather, A.E. Equilibrium between carbon dioxide and aqueous monoethamolamine solutions. Appl. Chem. Biotechnol. **1976**, *26*, 541–549.
3. Lee, J.I.; Otto, F.D.; Mather, A.E. The solubility of H_2S and CO_2 in aqueous monoethanolamine solutions. Can. J. Chem. Eng. **1974**, *52*, 803–805.
4. Shen, K.-P.; Li, M.-H. Solubility of carbon dioxide in aqueous mixtures of monoethanolamine with methyldiethanolamine. J. Chem. Data **1992**, *37*, 96–100.
5. Astarita, G. Carbon dioxide absorption in aqueous ethanolamine solutions. Chem. Eng. Sci. **1961**, *16*, 202–207.
6. Danckwerts, P.V.; Sharma, M.M. The absorption of carbon dioxide into solutions of alkalis and amines. Chem. Eng. **1966**, *10*, 244–280.
7. Donaldson, T.L.; Nguyen, Y.N. Carbon dioxide reaction kinetics and transport in aqueous amine membranes. Ind. Eng. Chem. Fund. **1980**, *19*, 260–266.
8. Hikita, H.; Asai, S.; Ishikawa, H.; Honda, M. The kinetics of reactions of carbon dioxide with monoethanolamine, diethanolamine and triethanolamine by a rapid mixing method. Chem. Eng. J. **1977**, *13*, 7–12.
9. Laddha, S.S.; Danckwerts, P.V. Reaction of carbon dioxide with ethanolamines: kinetics from gas-absorption. Chem. Eng. Sci. **1981**, *36*, 479–482.
10. Xu, G.-W.; Zhang, C.-F.; Qin, S.-J.; Gao, W.-H.; Liu, H.-B. Gas–liquid equilibrium in CO_2–MDEA-H_2O system and the effect of piperazine on it. Ind. Eng. Chem. Res. **1998**, *37*, 1473–1477.
11. Xu, G.-W.; Zhang, C.-F.; Qin, S.-J.; Wang, Y.-W. Kinetics study on absorption of carbon dioxide into solutions of activated methyldiethanolamine. Ind. Eng. Chem. Res. **1992**, *31*, 921–927.

12. Xu, G.-W.; Zhang, C.-F.; Qin, S.-J.; Zhu, B.-C. Desorption of CO_2 from MDEA and activated MDEA solution. Ind. Eng. Chem. Res. **1995**, *34*, 874–880.
13. Kaganoi, S. Carbon dioxide absorption in methyldiethanolamine with piperazine or diethanolamine: thermodynamics and rate measurements. MS Thesis, The University of Texas at Austin, 1997.
14. Bishnoi, S.; Rochelle, G.T. Absorption of carbon dioxide into aqueous piperazine: reaction kinetics, mass transfer and solubility. Chem. Eng. Sci. **2000**, *55*, 5531–5543.
15. Mshewa, M. Carbon dioxide desorption/absorption with aqueous mixture of methyldiethanolamine and diethanolamine at 40°C to 120°C. PhD Dissertation, The University of Texas at Austin, 1995.
16. Pacheco, M.A. Mass transfer, kinetics and rate-based modeling of reactive absorption. PhD Dissertation, The University of Texas at Austin, 1998.
17. Pacheco, M.A.; Kaganoi, S.; Rochelle, G.T. CO_2 absorption into aqueous mixtures of Diglycolamine® and methyldiethanolamine. Chem. Eng. Sci. **2000**, *55*, 5125–5140.
18. Dang, H.Y. Carbon dioxide absorption rate and solubility in monoethanolamine/piperazine/water. MS Thesis, The University of Texas at Austin, May 2001.
19. Bishnoi, S. Carbon dioxide absorption and solution equilibrium in piperazine activated methyldiethanolamine. PhD Dissertation, The University of Texas at Austin, December 2000.
20. Maurer, G. On the solubility of volatile weak electrolytes in aqueous solutions. *Thermodynamics of Aqueous Systems with Industrial Applications*; ACS Symp. Ser. 133; American Chemical Society: Washington, DC, 1980; 139–186.
21. Edwards, T.J.; Mauer, G.; Newman, J.; Prausnitz, J.M. Vapor–liquid equilibria in multicomponent aqueous solution of volatile weak electrolytes. AICHE J. **1978**, *24* (6), 966–976.
22. Bishnoi, S. Physical and chemical solubility of carbon dioxide in aqueous methyldiethanolamine. MS Thesis, The University of Texas at Austin, December 1998.
23. Weiland, R.H.; Dingman, J.C.; Cronin, D.B.; Browning, G.J. Density and viscosity of some partial carbonated aqueous alkanolamine solutions and their blends. J. Chem. Eng. Data **1998**, *43*, 378–382.
24. Licht, S.E.; Weiland, R.H. Density and physical solubility of carbon dioxide in partial-loaded solution of MEA, DEA, and MDEA and their blends. Spring National Meeting of the American Institute of Chemical Engineers, Houston, TX, Apr 2–6, 1989.

25. Versteeg, G.F.; van Swaaij, W.P.M. Solubility and diffusivity of acid gas (CO_2, N_2O) in aqueous alkanolamine solutions. J. Chem. Eng. Data. **1988**, *33*, 29–34.
26. Pigford, R.L. Counter-diffusion in a wetted wall column. PhD Dissertation, The University of Illinois: Urbana, Illinois, 1941.
27. Bates, R.G.; Pinching, G.D. Acidic dissociation constant and realated thermodynamic quantity for MEA ion in water from 0° to 50°C. J. Res. Nat. Bur. Stand., **1985**, *46* (5), 349–356.
28. Austgen, M.D.; Rochelle, G.T. Model of vapor–liquid equilibrium for aqueous acid gas-alkanolamine system using electrolyte-NRTL equation. IEC Res. **1989**, *28*, 1060–1073.

Received September 2001
Revised June 2002